• Clinical Research •

Quantitative analysis of posterior chamber morphology on vault after ICL implantation: a retrospective paired study

Qiu-Jian Zhu, Lie Ma, Hong Qian, Wei-Jian Zhu, You Yuan, E Song

Department of Ophthalmology, Lixiang Eye Hospital of Soochow University, Suzhou 215031, Jiangsu Province, China

Correspondence to: You Yuan and E Song. Department of Ophthalmology, Lixiang Eye Hospital of Soochow University, Suzhou 215031, Jiangsu Province, China. yuanyou@suda.edu.cn; songe@suda.edu.cn

Received: 2025-05-08 Accepted: 2025-08-11

Abstract

● **AIM:** To quantitatively evaluate the influence of four posterior chamber morphological features—wide iris-ciliary angle (ICA), concave iris (CI), anteriorly positioned ciliary body (APCB), and ciliary body cyst (CBC)—on vault after implantable Collamer lens (ICL) implantation.

● **METHODS:** In this retrospective paired study, 925 eyes from 506 patients were analyzed. Participants were matched 1:1 based on ICL size, horizontal/vertical sulcus-to-sulcus (STS) diameters, and lens thickness. Posterior chamber morphology was assessed using ultrasound biomicroscopy (UBM). Actual vault measurements were compared against vault values predicted using the Zhu formula. Statistical analyses included paired *t*-tests and Bland-Altman agreement assessment.

● **RESULTS:** Eyes with wide ICA (n=82) and CI (n=26) exhibited significantly lower actual vault (mean difference: −137.93 and −145.00 μm, respectively; P<0.001) compared to controls. Conversely, the APCB group (n=77) showed higher vault (mean increase: 222.60 μm; P<0.001), while CBC (n=36) had no significant impact (P=0.054). Bland-Altman analysis revealed systematic prediction errors: wide ICA and CI groups had underestimated vault (mean bias: −165.4 and −175.0 μm), whereas APCB showed overestimation (mean bias: +212.4 μm). Notably, 31.71% of wide ICA and 36.36% of APCB cases exceeded prediction errors of ±300 μm.

● **CONCLUSION:** Posterior chamber morphology, particularly wide ICA, CI, and APCB, significantly affects postoperative vault. These features introduce systematic deviations in vault prediction, highlighting the need for integrating morphological parameters into ICL sizing algorithms to optimize surgical outcomes and reduce complications.

● **KEYWORDS:** implantable Collamer lens; postoperative vault; posterior chamber morphology; ultrasound biomicroscopy; vault prediction

DOI:10.18240/ijo.2026.06.14

Citation: Zhu QJ, Ma L, Qian H, Zhu WJ, Yuan Y, Song E. Quantitative analysis of posterior chamber morphology on vault after ICL implantation: a retrospective paired study. *Int J Ophthalmol* 2026;19(6):1132-1139

INTRODUCTION

Implantable Collamer lens (ICL) implantation is a refractive surgery for correcting myopia [up to −18 diopter (D)] and astigmatism (up to −6 D)[1]. Its advantages, including corneal tissue preservation, minimal induction of high-order aberrations, and reversibility, make it a preferred option for patients with high myopia or abnormal corneal morphology[2]. The effectiveness, safety, and stability of ICL implantation have been confirmed by numerous studies[3-6]. Postoperative vault—the distance between the posterior ICL surface and the anterior crystalline lens—remains a critical parameter in ICL surgery. Excessive vault (≥750 μm) may precipitate acute angle-closure glaucoma, while insufficient vault (≤250 μm) increases the risk of anterior subcapsular cataracts[7-9]. Although ICL size selection is the primary controllable determinant of vault, current sizing algorithms rely on anterior segment parameters such as white-to-white (WTW) diameter and anterior chamber depth (ACD), which inadequately reflect the anatomy of posterior chamber where ICL located.

Moreover, several predictive formulas for postoperative vault estimation have recently been developed, including the Zhu formula established by our team[10-15]. However, none have proven to be flawless, as a subset of patients still demonstrate clinically significant vault deviations[16]. Recent studies highlight the influence of posterior chamber morphology on vault. A study conducted by Yang *et al*[17] revealed that concave iris (CI) morphology correlated with low vault, whereas convex iris morphology was linked to high vault in eyes with

thick lenses. Consistently, Ahmad Khan *et al*[18] demonstrated that eyes exhibiting markedly CI morphology linked to higher incidence of excessively low vault. On the other hand, several recent studies have indicated that the iris-ciliary angle (ICA) is associated with the postoperative vault after ICL surgery[19-21].

In our previous research, four posterior chamber morphology features that might significantly affect the accuracy of our prediction formula: wide ICA, CI, anteriorly positioned ciliary body (APCB), and ciliary body cyst (CBC)[15]. However, quantitative evidence linking specific posterior chamber features to vault remains limited. This study aims to investigate the influence of four posterior chamber morphological characteristics on postoperative vault following ICL implantation *via* a strict 1:1 matching protocol.

PARTICIPANTS AND METHODS

Ethics Approval This retrospective study was approved by the Ethics Committee of the Lixiang Eye Hospital of Soochow University (LXEH-2020-012) and adhered to the principles of the Helsinki Declaration. All subjects provided informed consent.

Study Design and Participants All subjects were consecutively enrolled from the Refractive Surgery Center of Lixiang Eye Hospital between July 1, 2020, and January 30, 2021. A total of 925 eyes from 506 subjects were included in this study. There were 204 males and 302 females, with an average age of 27.07±6.17y. The preoperative ultrasound biomicroscopy (UBM) examination results of all subjects were retrospectively reviewed.

Inclusion criteria for this study were subjects aged 18 to 45y with spherical equivalents (SE) of −0.50 to −18.00 diopter sphere (DS) and astigmatism up to −6.00 diopter cylinder (DC), stable refractive error or myopia progression <0.5 D/year for two years, endothelial cell density ≥2000 cells/mm², and ACD ≥2.8 mm. Exclusion criteria included uncontrolled keratoconus, corneal or endothelial dystrophy, severe dry eye, infections, glaucoma, cataracts, other ocular diseases, uveitis, fundus diseases affecting vision, severe mental illnesses, and systemic diseases such as diabetes, uncontrolled thyroid dysfunction, autoimmune diseases, or long-term immunosuppressant use.

Selection of UBM Image Features The UBM (SW-3200 L; SUOER, Tianjin, China) device in this study is equipped with a 50 MHz high-frequency sensing ultrasound probe, with a lateral and longitudinal resolution of 40 μm. In the panoramic mode, the scanning range can be as wide as 17 mm, and the depth can reach 10 mm. During the examination, the patient lies flat on the examination bed. After topical anesthesia, an appropriate eye cup is placed in the conjunctival sac of the examined eye, and an appropriate amount of normal saline is poured into the eye cup, and then the ultrasound probe is used for examination. The patient is asked to look at a target on the ceiling 4 meters above to relax the accommodation. The eye cross-sectional images in the horizontal direction (3–9 o'clock) and the vertical direction (12–6 o'clock) are measured, and the images with clear visualization of the corneal and lenticular surfaces and the ciliary sulcus distance is the largest are selected for this part of the study. In addition, local ciliary sulcus cross-sectional images in the four directions of up, down, nasal, and temporal of each eye are additionally examined under dynamic conditions. In summary, six images of each eye are included in this study.

All UBM images were imported into a personal computer and viewed and analyzed one by one using ImageJ. Cases with all four features were selected and marked. To minimize subjectivity, all UBM features were independently assessed by two researchers (Zhu WJ and Qian H). Discrepancies were resolved by a third adjudicator (Zhu QJ). The specific features are as follows: wide iris-ciliary angle, CI, APCB, and CBC. The details are as follows.

Wide ICA The ICA refers to the angle between the posterior surface of the iris and the anterior surface of the ciliary body. If this angle is greater than or equal to 90°, we consider this feature as a wide ICA (Figure 1A).

Concave iris A CI means that the iris is recessed backward, which can also be described as the central point of the posterior surface of the iris being significantly lower than the line connecting the two ends (Figure 1B).

Anteriorly positioned ciliary body We adopted Sakata *et al*'s[22] definition of the APCB. It refers to the condition where the ciliary processes of the ciliary body hypertrophy and extend into the ciliary sulcus, and in at least two quadrants, the root of the posterior surface of the iris is in contact with the hypertrophied ciliary processes or the posterior chamber angle disappears (ICA=0°; Figure 1C).

Ciliary body cyst A CBC refers to a cystic or hollow change inside the ciliary body. As shown in Figure 1D.

Match Protocol The subjects in each feature group were paired 1:1 according to the ICL size, horizontal sulcus-to-sulcus (STS) diameter, lens thickness (LT), vertical STS, laterality and gender. When pairing, the implanted ICL size, laterality and gender must be exactly the same, and the difference in the other three parameters should be within 0.2 mm during pairing.

Predicted vault is referred to as the vault calculated by the Zhu formula established by our team (central vault (μm)=−1369.05+657.121×ICL size-287.408×horizontal STS-432.497×crystalline LT-137.33×vertical STS)[14-15]. The differences between each feature group and the control group, as well as the differences between the actual vault and the predicted vault of the feature group, were compared.

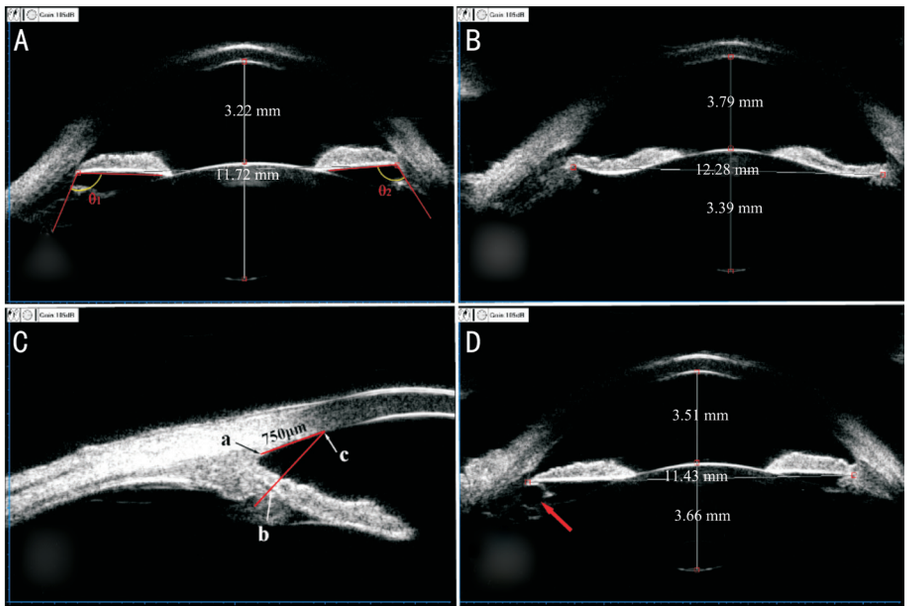

Figure 1 Four UBM features that may affect ICL vault A: Wide ICA, angles θ1 and θ2 between the posterior iris surface and the anterior surface of the ciliary body measuring greater than 90°; B: CI, in which the iris bows backwards; C: APCB, Sakata *et al*'s[22] definition of the APCB was adopted in this study. (b) is a point of the corneal endothelium 750 μm from the scleral spur (a), a line is drawn from (b) perpendicular to the posterior surface of the iris, intersects with the points (c), between (c) and the iris root, the ciliary body and iris contact, and the ciliary sulcus disappears; D: CBC, the red arrow points to the CBC. The figure legend is consistent with our previous study[15]. UBM: Ultrasound biomicroscopy; ICL: Implantable Collamer lens; ICA: Iris-ciliary angle; CI: Concave iris; APCB: Anteriorly positioned ciliary body; CBC: Ciliary body cyst.

Statistical Analysis The normality of all continuous variables was assessed using the Kolmogorov-Smirnov test. Normally distributed data were presented as mean±standard deviation (SD), while non-normally distributed data were summarized as median with interquartile range. Comparisons between the feature group and control group were conducted using paired *t*-tests, with results reported as mean differences, SD of differences, and 95% confidence intervals. The agreement between actual vault measurements and predicted vault values in the feature group was evaluated through Bland-Altman analysis, including calculation of mean differences and 95% limits of agreement (95% LoA). All statistical analyses were performed using SPSS software (version 22.0; IBM Corp., Armonk, NY, USA), with a two-tailed P value<0.05 considered statistically significant.

RESULTS

Finally, 82 eyes with a wide ICA (8.86% of the total), 26 eyes with a CI (2.81% of the total), 77 eyes with an APCB (8.32% of the total), and 36 eyes with a CBC (3.89% of the total) were screened out. The baseline data of each feature group are shown in Table 1.

As shown in Table 2 and Table 3, the actual vault in the Wide ICA and CI groups was 366.46±177.72 and 372.31±147.60 μm, respectively, which were significantly lower than those in the control group (504.39±167.07 and 517.31±148.98 μm; P<0.001 and P=0.001, respectively), with the difference −137.93±241.78 and −145.00±190.69 μm, respectively. In contrast, the APCB group exhibited a significantly higher actual vault (694.81±199.98 μm) compared to the control group (472.21±179.57 μm; P<0.001), with the difference 222.60±273.77 μm. However, no statistically significant difference in actual vault was observed between the CBC group and the control group (P=0.054). Except for the CBC and APCB groups, no significant differences were detected in predicted vault, horizontal STS, vertical STS, or LT between the remaining three feature groups and the control group (all P>0.05). Notably, there were no statistically significant differences in age, WTW, or ACD between the feature groups and the control group across the four subject groups (all P>0.05).

Bland-Altman plots were utilized to assess the agreement between actual and predicted vault measurements across four study groups (Figure 2). The Wide ICA group demonstrated a mean bias of −165.4 μm (SD ±194.5) with 95% LoA ranging from −546.6 to 215.9 μm. Similarly, the CI group showed a mean difference of −175.0 μm (SD ±159.2) and 95% LoA between −487.5 and 136.6 μm. In contrast, the APCB group exhibited a positive mean bias of 212.4 μm (SD ±183.0) with wider 95% LoA spanning from −146.2 to 571.0 μm. The CBC group displayed the smallest systematic bias (mean difference 42.06 μm, SD ±203.5), though its 95% LoA extended from −356.8 to 440.9 μm, indicating comparable variability to other groups.

Figure 3 presents the distribution of prediction errors for each feature group. For the wide ICA group, predictions

Table 1 Baseline data for the four feature groups mean±SD

Parameters	Wide ICA	CI	APCB	CBC	*P*
Number	82	26	77	36	
Age, y	29.15±6.66	29.07±6.70	26.92±5.67	26.53±4.84	0.270
Gender, F/M	47/35	11/15	36/31	26/10	0.303
Actual vault, μm	366.46±177.72	372.31±147.60	694.81±199.98	556.11±232.11	<0.001
WTW, mm	11.51±0.41	11.64±0.43	11.67±0.42	11.74±0.48	0.011
Horizontal STS, mm	11.44±0.39	11.62±0.47	11.53±0.41	11.59±0.42	0.067
Vertical STS, mm	11.83±0.39	12.07±0.47	11.93±0.43	11.99±0.50	0.056
ACD, mm	3.28±0.26	3.30±0.22	3.28±0.25	3.30±0.25	0.820
K1, D	43.18±1.30	42.72±1.32	42.97±1.51	42.90±1.71	0.285
K2, D	44.74±1.44	44.10±1.77	44.63±1.62	44.46±1.82	0.285
AL, mm	26.80±1.07	27.04±1.62	26.71±1.42	26.66±1.30	0.436
LT, mm	3.74±0.28	3.78±0.28	3.66±0.21	3.68±0.24	0.044
SE, D	−8.33±2.07	−8.05±2.99	−8.04±2.86	−7.91±2.83	0.910
ICL size, 12.1/12.6/13.2/13.7 mm	4/43/35/0	0/10/14/2	7/43/27/0	3/15/18/0	

ICA: Iris-ciliary angle; CI: Concave iris; APCB: Anteriorly positioned ciliary body; CBC: Ciliary body cyst; WTW: White-to-white diameter; STS: Sulcus-to-sulcus diameter; ACD: Anterior chamber depth; AL: Axial length; LT: Lens thickness; SE: Spherical equivalent. F: Female; M: Male; SD: Standard deviation.

Table 2 Comparative analysis of each feature group and the control group mean±SD

Parameters	Wide ICA			CI		
	Feature group	Control group	*P*	Feature group	Control group	*P*
Actual vault, μm	366.46±177.72	504.39±167.07	<0.001	372.31±147.60	517.31±148.98	0.001
Predicted vault, μm	531.82±91.28	528.13±87.19	0.611	547.59±93.28	531.56±90.97	0.183
Horizontal STS, mm	11.44±0.39	11.43±0.39	0.303	11.62±0.47	11.60±0.44	0.181
Vertical STS, mm	11.83±0.39	11.85±0.38	0.202	12.07±0.47	12.13±0.54	0.120
LT, mm	3.74±0.28	3.75±0.27	0.326	3.78±0.28	3.78±0.26	0.838
Age, y	29.15±6.66	28.91±6.47	0.747	29.07±6.70	28.23±7.56	0.560
WTW, mm	11.51±0.41	11.52±0.38	0.733	11.64±0.43	11.61±0.39	0.707
ACD, mm	3.28±0.26	3.26±0.23	0.469	3.30±0.22	3.24±0.20	0.216

ICA: Iris-ciliary angle; CI: Concave iris; STS: Sulcus-to-sulcus diameter; LT: Lens thickness; WTW: White-to-white diameter; ACD: Anterior chamber depth; SD: Standard deviation.

Table 3 Comparative analysis of each feature group and the control group mean±SD

Parameters	APCB			CBC		
	Feature group	Control group	*P*	Feature group	Control group	*P*
Actual vault, μm	694.81±199.98	472.21±179.57	<0.001	556.11±232.11	480.83±165.38	0.054
Predicted vault, μm	482.39±97.86	480.08±96.45	0.498	514.08±104.07	505.77±95.62	0.088
Horizontal STS, mm	11.53±0.41	11.52±0.40	0.005	11.59±0. 42	11.59±0.40	0.850
Vertical STS, mm	11.93±0.43	11.95±0.42	0.382	11.99±0.50	12.00±0.48	0.017
LT, mm	3.66±0.21	3.67±0.19	0.208	3.68±0.24	3.68±0.25	0.342
Age, y	26.92±5.67	26.84±6.18	0.911	26.53±4.84	28.42±6.02	0.069
WTW, mm	11.67±0.42	11.63±0.36	0.326	11.74±0.48	11.62±0.32	0.053
ACD, mm	3.28±0.25	3.24±0.21	0.144	3.28±0.26	3.27±0.24	0.802

APCB: Anteriorly positioned ciliary body; CBC: Ciliary body cyst; STS: Sulcus-to-sulcus diameter; LT: Lens thickness; WTW: White-to-white diameter; ACD: Anterior chamber depth; SD: Standard deviation.

were overestimated in 66 cases (80.48%), with 26 cases (31.71%) showing overestimations exceeding 300 μm, while underestimations occurred in 16 cases (19.51%). In the CI group, predictions were overestimated in 22 cases (84.62%), including 7 cases (26.92%) with overestimations exceeding 300 μm, and underestimations were observed in 4 cases (15.38%). For the APCB group, predictions were overestimated in 12 cases (15.58%), while underestimations

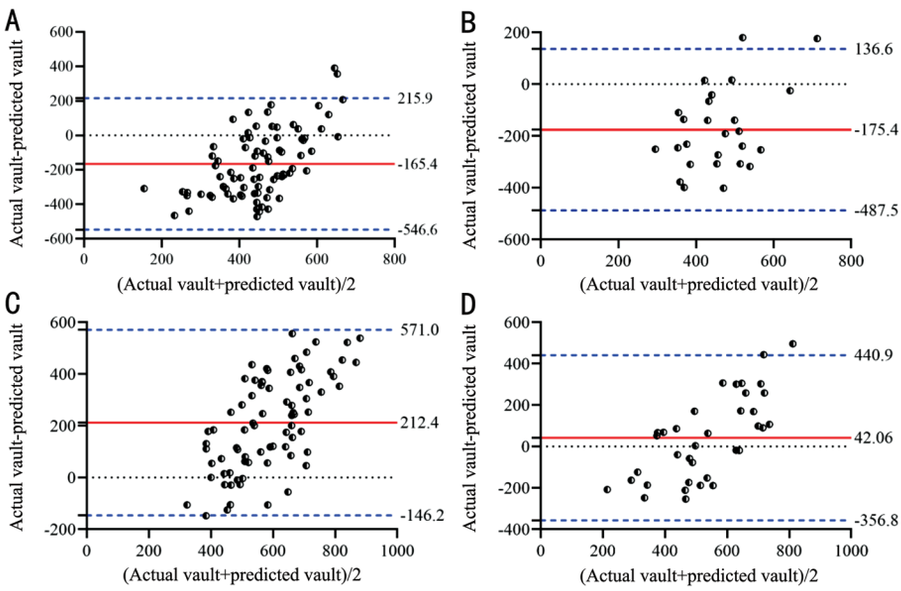

Figure 2 Bland-Altman plots were utilized to assess the agreement between actual and predicted vault measurements across four study groups A: Wide ICA; B: CI; C: APCB; D: CBC. The red solid line represents the mean difference, while the blue dashed line denotes the 95% LoA. ICA: Iris-ciliary angle; CI: Concave iris; APCB: Anteriorly positioned ciliary body; CBC: Ciliary body cyst; LoA: Limits of agreement.

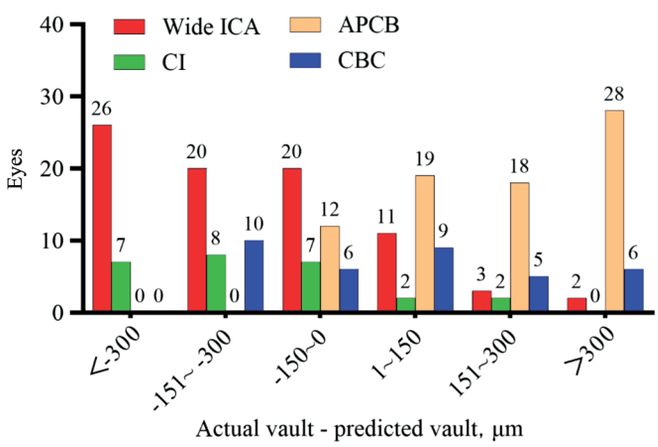

Figure 3 Distribution of prediction errors in the four feature groups ICA: Iris-ciliary angle; CI: Concave iris; APCB: Anteriorly positioned ciliary body; CBC: Ciliary body cyst.

occurred in 65 cases (84.42%), with 28 cases (36.36%) showing underestimations exceeding 300 μm. In the CBC group, predictions were overestimated in 16 cases (44.44%) and underestimated in 20 cases (55.56%), with 6 cases (16.67%) demonstrating underestimations exceeding 300 μm.

DISCUSSION

This study quantitatively evaluated the impact of four posterior chamber morphological features—wide ICA, CI, APCB, and CBC—on postoperative vault after ICL implantation. Our findings revealed that eyes with wide ICA or CI exhibited significantly lower vault (mean reductions: 137.9 μm or 145.0 μm, respectively) compared to matched controls, while APCB was associated with higher vault (mean increase: 222.6 μm). CBC did not significantly influence vault. These results highlight the critical role of posterior chamber anatomy in optimizing ICL sizing and vault prediction.

Since the introduction of ICL surgery, achieving optimal postoperative vault has remained a primary objective for both surgeons and researchers. Over the past decade, numerous predictive methods and formulas for vault estimation have been developed[23]. Nevertheless, instances of extremely inappropriate vault (either excessive or insufficient) continue to occur unexpectedly[7]. This persistent challenge may stem from a fundamental limitation inherent in current prediction methodologies: all existing vault prediction formulas rely exclusively on one-dimensional measurement parameters, essentially linear dimensions of ocular structures. Specifically, the ciliary sulcus-the actual anatomical site for ICL positioning-constitutes a three-dimensional structure that current imaging modalities cannot fully characterize. Although existing technologies cannot provide three-dimensional visualization of the sulcal anatomy, we hypothesize that incorporating two-dimensional morphological parameters might offer more comprehensive sulcus characterization and consequently improve postoperative vault predictability. This dimensional expansion in parameter selection could potentially address the current limitations in vault prediction accuracy. The posterior chamber is anatomically defined by three principal boundaries: the posterior iris surface anteriorly, the ciliary body and zonular fibers laterally/posteriorly, and the peripheral lens capsule posteriorly. Current evidence suggests that the morphological characteristics of each constituent structure (iris configuration and sulcus dimensions) are recognized as potential biomechanical determinants influencing ICL vault.

Recently, emerging evidence suggests that specific morphological features of the posterior chamber may serve as critical determinants of postoperative vault. Chen *et al*[21] demonstrated that anterior ciliary body displacement significantly increases the risk of excessive vault following ICL implantation, with a dose-dependent relationship observed whereby each 1° reduction in ICA elevates the odds of vault exceeding 1000 μm by 4% [adjusted odds ratio (OR)=0.96, 95% confidence intervals: 0.93–0.99; *P*<0.001]. Similarly, a recent study by Ni *et al*[20] reported an inverse correlation between ICA and postoperative vault, with the wide ICA group (>60°) exhibiting the lowest vault values, followed by normal (40°–60°) and narrow (<40°) groups; ordered multicategorical logistic regression analyses revealed significantly increased odds ratios for higher vault in narrower ICA groups (normal: OR=2.586, *P*=0.002; narrow: OR=5.534, *P*<0.001) using the wide ICA cohort as reference. On the other hand, Ahmad Khan *et al*[18] established a significant association between the obviously CI and a higher rate of excessively low vault (<100 μm). Consistently, Yang *et al*[17] demonstrated that CI configurations in eyes with thicker crystalline lenses predispose to insufficient vault, whereas convex iris profiles are associated with excessive vault. These findings are highly consistent with this study. However, the quantitative relationship between specific anatomical features and vault remains unestablished, necessitating further analyses to precisely delineate their contributions.

According to the present study, when predicting vault using the Zhu formula, subjects with wide ICA features exhibited a vault that was on average 165.4 μm lower than the predicted value and 137.9 μm lower than their paired controls. Similarly, subjects with CI features demonstrated a mean vault 175.0 μm below the predicted value and 145.0 μm lower than matched controls. In contrast, subjects with APCB features showed a mean vault exceeding predictions by 212.4 μm and surpassing controls by 222.6 μm. However, these values represent only mean differences, with substantial prediction deviations observed among individuals possessing these anatomical characteristics. For instance, in cases with wide ICA features, the 95% LoA for prediction errors spanned from −546.6 to 215.9 μm. Notably, 31.71% of these subjects exhibited actual vault measurements more than 300 μm below predictions, while 19.51% paradoxically demonstrated higher vault values than predicted. These findings highlight significant variability in prediction accuracy across individuals, suggesting a need for personalized preoperative assessments beyond linear parameters. Therefore, while these anatomical features demonstrate systematic trends in vault prediction deviations, their clinical interpretation requires caution.

The observed lower vault in wide ICA and CI groups may stem from altered spatial relationships between the ICL and surrounding structures. A wide ICA likely reduces resistance to posterior displacement of the ICL, allowing it to settle closer to the crystalline lens. Similarly, CI morphology may create a posteriorly directed force on the ICL haptics, further lowering the vault. Conversely, APCB, characterized by hypertrophied ciliary processes encroaching into the ciliary sulcus, could physically restrict ICL posterior movement, leading to excessive vault. These mechanisms align with prior studies suggesting that iris curvature and ciliary body morphology modulate ICL haptic positioning. Two recent studies by Tan *et al*[19,24] proposed the hypothesis that the final tip point of the ICL (ftICL) haptic was significantly associated with the ICA. Specifically, for each degree increase in the ICA, the ftICL haptic increased by 0.01 mm, ultimately leading to an increased likelihood of a higher vault. In other words, larger ICA correlates with inferior ftICL haptic positioning and lower postoperative vault, while smaller ICA associate with superior ftICL haptic placement and higher vault. Subjects exhibiting APCB features demonstrate near-zero ICA values, predisposing to elevated vault. The CBC group exhibited the highest SD (203.5 μm) in prediction errors and the widest 95% agreement interval (extended from −356.8 to 440.9 μm) among all groups. Consistent with prior studies, we still believe that the influence of CBCs on vault is related to their location[15,25-26]. Notably, in this study, one-sixth (16.7%) of CBC subjects displayed an actual vault exceeding predicted values by >300 μm.

The observed systematic biases and wide LoA are clinically significant as they directly relate to established safety thresholds for ICL vault. Current consensus suggests an optimal vault range of 250–750 μm, with vaults below 100 μm carrying a significant risk of anterior subcapsular cataract due to lens contact, and vaults exceeding 1000 μm posing a risk for pupillary block or angle-closure glaucoma. Crucially, our Bland-Altman analysis revealed that mean prediction biases (*e.g.*, −165.4 μm underestimation in Wide ICA, +212.4 μm overestimation in APCB) are substantial enough to push clinically targeted vault predictions (often aimed at the mid-range, *e.g.*, 500 μm) outside the optimal zone or close to critical thresholds. Furthermore, the wide 95% LoA (*e.g.*, −546.6 to 215.9 μm for Wide ICA) and the finding that 31.7% of Wide ICA and 36.4% of APCB cases exceeded prediction errors of ±300 μm, indicate a high likelihood of clinically significant deviations in individual patients. Such large errors could readily result in vaults <100 μm or >1000 μm if preoperative predictions do not account for these morphological features, necessitating ICL exchange or urgent intervention. These findings underscore the critical need to integrate posterior chamber morphology assessment (specifically Wide ICA, CI,

and APCB) into preoperative planning to mitigate the risk of vault-related complications.

This study has limitations. First, its retrospective design has inherent limitations, and the findings require validation through future prospective investigations. Second, although the sample size in this study is moderately large compared to similar investigations, more participants will be enrolled, especially the CI group, to strengthen the findings. Third, the vault prediction in this study was based on the Zhu formula, whose accuracy has been validated[15]. Although no statistically significant differences in WTW or ACD were observed between the feature subgroups and control group within each cohort, further research is required to determine the applicability of other vault prediction formulas. Furthermore, the posterior chamber features in this study were assessed solely *via* UBM, which requires specialized technical skills. Variability in anatomical sectioning, particularly during ICA measurements, may influence result interpretation and limit broader clinical applicability.

In conclusion, posterior chamber morphology, particularly wide ICA, CI, and APCB, significantly influences postoperative vault after ICL implantation. These features should be systematically evaluated during preoperative planning to optimize ICL sizing and minimize complications related to inadequate or excessive vault. Incorporating posterior chamber morphology into predictive models may enhance ICL sizing precision.

ACKNOWLEDGEMENTS

The authors would like to thank Xiao-Qin Ni for the data collection.

Authors' Contributions: Zhu QJ performed the statistical analysis and wrote the original draft. Yuan Y and Song E conceptualized the study; Qian H and Zhu WJ analyzed the UBM images and were responsible for data curation; Ma L modified the manuscript; All authors read, reviewed, and approved the final manuscript.

Availability of Data and Materials: The data used in this study can be requested by contacting the corresponding author.

Conflicts of Interest: Zhu QJ, None; **Ma L,** None; **Qian H,** None; **Zhu WJ,** None; **Yuan Y,** None; **Song E,** None.

REFERENCES

1 Packer M. The Implantable Collamer Lens with a central port: review of the literature. *Clin Ophthalmol* 2018;12:2427-2438.

2 Niu LL, Miao HM, Tian M, *et al*. One-year visual outcomes and optical quality of femtosecond laser small incision lenticule extraction and Visian Implantable Collamer Lens (ICL V4c) implantation for high myopia. *Acta Ophthalmol* 2020;98(6):e662-e667.

3 Chen X, Wang XQ, Xu YL, *et al*. Long-term comparison of vault and complications of implantable collamer lens with and without a central hole for high myopia correction: 5 years. *Curr Eye Res* 2022;47(4): 540-546.

4 Fernández-Vega-Cueto L, Alfonso-Bartolozzi B, Lisa C, *et al*. Seven-year follow-up of posterior chamber phakic intraocular lens with central port design. *Eye Vis (Lond)* 2021;8(1):23.

5 Chung B, Choi JY, Kang DSY, *et al*. Ten-year clinical outcomes of V4c implantable collamer lens implantation: longitudinal analysis of visual acuity, endothelial cell density, and vault dynamics. *Am J Ophthalmol* 2025;269:1-10.

6 Wannapanich T, Kasetsuwan N, Reinprayoon U. Intraocular implantable collamer lens with a central hole implantation: safety, efficacy, and patient outcomes. *Clin Ophthalmol* 2023;17:969-980.

7 Zhang PC, Guo CJ, Wang S, *et al*. Influencing factors comparing different vault groups after phakic implantable collamer lens implantation: review and meta-analysis. *BMC Ophthalmol* 2024;24(1):70.

8 Frost A, Ritter D, Trotter A, *et al*. Acute angle-closure glaucoma secondary to a phakic intraocular lens, an ophthalmic emergency. *Clin Pract Cases Emerg Med* 2019;3(2):137-139.

9 Yu YB, Zhang CS, Zhu YN. Femtosecond laser assisted cataract surgery in a cataract patient with a "0 vaulted" ICL: a case report. *BMC Ophthalmol* 2020;20(1):179.

10 Wu H, Zhong DJ, Luo DQ, *et al*. Improvement in the ideal range of vault after implantable collamer lens implantation: a new vault prediction formula. *Front Med (Lausanne)* 2023;10:1132102.

11 Kojima T, Yokoyama S, Ito M, *et al*. Optimization of an implantable collamer lens sizing method using high-frequency ultrasound biomicroscopy. *Am J Ophthalmol* 2012;153(4):632-637.e1.

12 Zhang J, Shao J, Zheng L, *et al*. Implantable collamer lens sizing based on measurement of the sulcus-to-sulcus distance in ultrasound biomicroscopy video clips and ZZ ICL formula. *BMC Ophthalmol* 2022;22(1):363.

13 Di Y, Li Y, Luo Y. Prediction of implantable collamer lens vault based on preoperative biometric factors and lens parameters. *J Refract Surg* 2023;39(5):332-339.

14 Zhu QJ, Chen WJ, Zhu WJ, *et al*. Short-term changes in and preoperative factors affecting vaulting after posterior chamber phakic Implantable Collamer Lens implantation. *BMC Ophthalmol* 2021;21(1):199.

15 Zhu QJ, Xing XY, Zhu MH, *et al*. Validation of the vault prediction model based on the sulcus-to-sulcus diameter and lens thickness: a 925-eye prospective study. *BMC Ophthalmol* 2022;22(1):463.

16 Wu H, Luo DQ, Chen J, *et al*. Comparison of the accuracy of seven vault prediction formulae for implantable collamer lens implantation. *Ophthalmol Ther* 2024;13(1):237-249.

17 Yang ZK, Meng LH, Zhao XY, *et al*. Clinical prediction of inadequate vault in eyes with thick lens after implantable collamer lens implantation using iris morphology. *Front Med (Lausanne)* 2022;9:906433.

18 Ahmad Khan M, Tan Q, Sun W, *et al*. Prediction of excessively low vault after implantable collamer lens implantation using iris morphology. *Front Med (Lausanne)* 2022;9:1029350.

19 Tan WN, Wang Z, Zeng QY, *et al*. The influence of iris-ciliary angle (ICA) on the vault after implantation of V4c implantable collamer lens: a chain mediation model of ICL haptic related factors. *BMC Ophthalmol* 2023;23(1):403.

20 Ni YJ, He SY, Jin HH, *et al*. Effect of the iris-ciliary angle on the prediction of the vault for phakic implantable collamer lens in the manufacturer's calculator. *BMC Ophthalmol* 2024; 24(1):491.

21 Chen Q, Tan WN, Lei XH, *et al*. Clinical prediction of excessive vault after implantable collamer lens implantation using ciliary body morphology. *J Refract Surg* 2020;36(6):380-387.

22 Sakata LM, Sakata K, Susanna R Jr, *et al*. Long ciliary processes with no ciliary sulcus and appositional angle closure assessed by ultrasound biomicroscopy. *J Glaucoma* 2006;15(5):371-379.

23 Thompson V, Cummings A, Wang XY. Implantable collamer lens procedure planning: a review of global approaches. *Clin Ophthalmol* 2024;18:1033-1043.

24 Tan WN, Chen Q, Yang RB, *et al*. Characteristics and factors associated with the position of the haptic after ICL V4C implantation. *J Cataract Refract Surg* 2023;49(4):416-422.

25 Zeng QY, Xie XL, Chen Q. Prevention and management of collagen copolymer phakic intraocular lens exchange: Causes and surgical techniques. *J Cataract Refract Surg* 2015;41(3):576-584.

26 Li Z, Xu ZK, Wang YQ, *et al*. Implantable collamer lens surgery in patients with primary iris and/or ciliary body cysts. *BMC Ophthalmol* 2018;18(1):287.